*Earth Planets Space*, **64**, 1239–1243, 2012

# Coulomb stress change for the normal-fault aftershocks triggered near the Japan Trench by the 2011 $M_w$ 9.0 Tohoku-Oki earthquake

Tamao Sato[1], Shinya Hiratsuka[1], and Jim Mori[2]

[1]*Department of Earth and Environmental Sciences, Hirosaki University, Hirosaki, Japan*
[2]*Disaster Prevention Research Institute, Kyoto University, Kyoto, Japan*

(Received December 27, 2011; Revised March 19, 2012; Accepted April 6, 2012; Online published January 28, 2013)

Coulomb stress triggering is examined using well-determined aftershock focal mechanisms and source models of the 2011 $M_w$ 9.0 off the Pacific coast of Tohoku Earthquake. We tested several slip distributions obtained by inverting onshore GPS-derived coseismic displacements under different *a priori* constraints on the initial fault parameters. The aftershock focal mechanisms are most consistent with the Coulomb stress change calculated for a slip distribution having a center of slip close to the trench. This demonstrates the capability of the Coulomb stress change to help constrain the slip distribution that is otherwise difficult to determine. Coulomb stress changes for normal-fault aftershocks near the Japan Trench are found to be strongly dependent on the slip on the shallow portion of the fault. This fact suggests the possibility that the slip on the shallow portion of the fault can be better constrained by combining information of the Coulomb stress change with other available data. The case of normal-fault aftershocks near some trench segment which are calculated to be negatively stressed shows such an example, suggesting that the actual slip on the shallow portion of the fault is larger than that inverted from GPS-derived coseismic displacements.

**Key words:** Off the Pacific coast of Tohoku Earthquake, Tohoku-Oki earthquake, Coulomb stress change, giant earthquake, slip near the trench, outer rise, Japan Trench.

## 1. Introduction

The 2011 $M_w$ 9.0 off the Pacific coast of Tohoku Earthquake (hereafter, '2011 Tohoku-Oki earthquake') occurred along the western margin of the Pacific Ocean where the Pacific plate is subducted beneath the island of Honshu, Japan. The earthquake triggered an intense aftershock activity in and around the mainshock fault zone (Hirose *et al*., 2011). Toda *et al*. (2011) examined the Coulomb stress triggering hypothesis using 177 NIED F-net aftershock focal mechanisms. They tested six source models obtained from seismic, geodetic, and tsunami observations, and showed that there was a significant gain in positively-stressed aftershock mechanisms over that for the background earthquakes. However, the six source models all assume planar fault planes with a constant dip angle in the range of 9–15 degrees. This assumption may be too simple to evaluate the change in the Coulomb Failure Function (hereafter, '$\Delta$CFF' or 'Coulomb stress change') of an aftershock near the mainshock fault, because the precise location of an aftershock relative to the mainshock fault is required for evaluating its Coulomb stress change accurately.

In this paper, we examine the Coulomb stress triggering, using well-determined aftershock focal mechanisms and slip distributions of the 2011 Tohoku-Oki earthquake inverted from GPS-derived coseismic displacements on land. The fault geometry is constructed on an accurate three-dimensional configuration of the upper plate interface of the subducted Pacific plate. We test the fault models against the aftershock focal mechanisms determined by Nettles *et al*. (2011), which are considered to be more accurate than others determined on a routine basis. Based on the calculated $\Delta$CFF, we assess the capability of the Coulomb stress change to help constrain the slip distribution; which is difficult to determine from the GPS-derived coseismic displacements.

## 2. Fault Model

In modeling the fault geometry of the 2011 Tohoku-Oki earthquake, we refer to the depths of the upper plate interface of the subducted Pacific plate determined by Takeuchi *et al*. (2008). These depths were determined using both the earthquake distribution and offshore crustal structures revealed by seismic experiments. We set 114 rectangular fault segments on the plate interface to form the entire fault surface of the Tohoku-Oki earthquake (Fig. 1). The upper end of the fault is set at a depth of 6.5 km beneath the axis of the Japan Trench. The lower end of the fault is set at a depth of 50 km. The fault is segmented at depths of 10, 15, 20, 30, and 40 km in the dip direction. The lengths of fault segments in the strike direction are in the range of 30–40 km. The orientation of each fault segment is fitted to the local strike and dip of the plate interface.

We use the coseismic displacements derived from the GPS measurements of GEONET (Fig. 2) to determine the slip distribution on the fault. Although the geodetic data



doi:10.5047/eps.2012.04.003

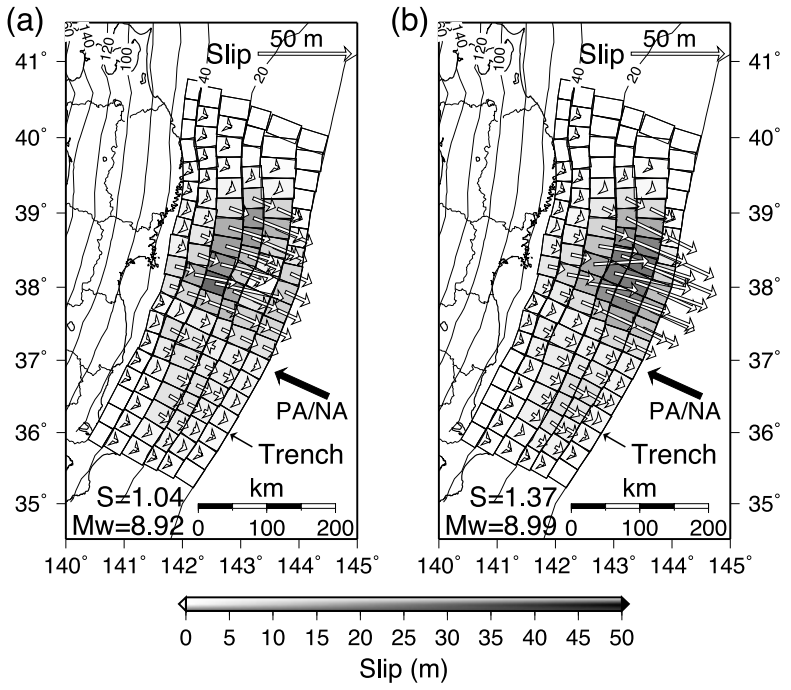


Fig. 1. (a) Inverted slip distribution obtained under a weak constraint given by a standard deviation of 30% of the initial slip, and (b) the same under a strong constraint given by a standard deviation of 7% of the initial slip. The arrows indicate the slip vectors. The thick arrow indicates the direction of motion of the Pacific plate relative to the North American plate. The contours denote the depths of plate interface at 20-km intervals. S indicates the variance of weighted residuals, and $M_w$ the moment magnitude.

is the same as that used by Ozawa *et al*. (2011), the slip distribution will not be the same because the fault geometry differs. Here, we only use two horizontal components, assuming their standard errors to be 10 mm. We do not use vertical components since their errors are estimated to be larger than those of the horizontal components, although it is confirmed that the inclusion of vertical components does not affect the results significantly. The static displacements and strains due to the slip on the fault are calculated using the source code developed by Okada (1992) for a half-space medium. The Poisson ratio of the homogeneous medium is assumed to be 0.25.

Inversions of the GPS-derived displacements were performed using the program system 'SALS' developed for nonlinear least-squares fitting in experimental sciences (Nakagawa and Oyanagi, 1980). We adopted a generalized inversion method in which the solutions are determined under different *a priori* strengths of constraints on initial unknown parameters. The unknowns are the slips and rakes for all fault segments. We assume an initial slip distribution that looks similar to that obtained from tsunami data by Fujii *et al*. (2011), in the sense that the maximum, or center of, slip is close to the trench. We assume the initial slip direction to be parallel to the direction of motion of the Pacific plate relative to the North American plate (Altamimi *et al*., 2007). The constraint on the initial rake was uniformly specified by a standard deviation of 6 degrees. For the constraint on the slip, we tested several standard deviations in the range of 7–30% of the initial slip. As we increase the standard deviation on the initial slip, i.e. with weakening constraint on the initial slip, the center of slip systematically migrates from the shallow portion of the fault close to

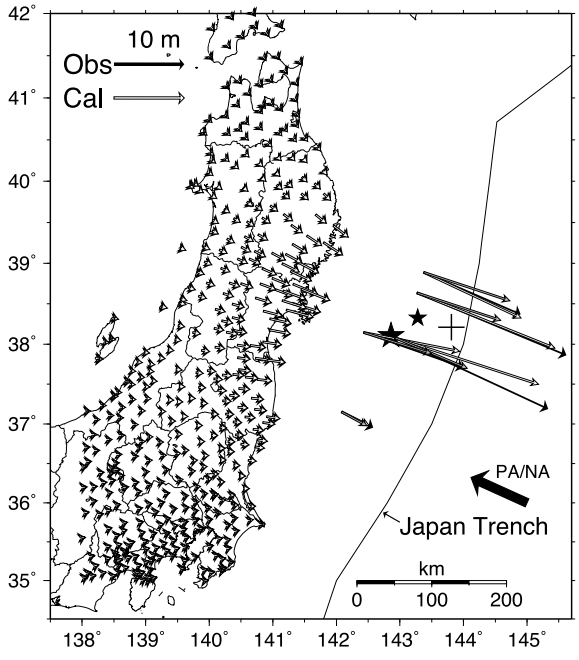


Fig. 2. Distribution of GPS stations of GEONET used for determining the slip distribution of the fault. The observed displacements (solid arrow) are compared with the displacements calculated (open arrows) for the slip distribution with the center of slip close to the trench (Fig. 1(b)). The observed displacements at the ocean-bottom observation sites (Sato *et al*., 2011) are also shown together with the calculated ones. The gray arrows are the displacements calculated for the slip distribution with the center of slip distant from the trench (Fig. 1(a)). Large and small stars indicate the epicenters of the $M_w$ 9.0 Tohoku-Oki earthquake and the $M_w$ 7.3 foreshock, respectively. The cross denotes the ocean-bottom observation site near the trench where an extremely large displacement is observed (Ito *et al*., 2011).

the trench toward the deeper portion away from the trench. Figure 1 shows the results obtained for the two end members. The variance of weighted residuals for the fault model with the center of slip distant from the trench (Fig. 1(a)) is 24% smaller than that for the fault model with the center of slip close to the trench (Fig. 1(b)). The GEONET data fit better a slip distribution with the center of slip distant from the trench. However, as shown in Fig. 2, the ocean-bottom displacements observed by Sato *et al.* (2011) are a better fit to the slip distribution with the center of slip close to the trench. The slip distribution with the center of slip distant from the trench cannot explain the large displacements observed at those ocean-bottom sites. This inconsistency may be ascribed to the modeling based on a homogeneous half-space medium. The half-space modeling may be insufficient for dealing with observations extending over epicentral distances up to several hundred kilometers. Whatever the reason for the inconsistency, the model with the center of slip close to the trench is considered to be preferable because an extremely large slip on a shallow plate boundary is suggested by large crustal deformations observed near the trench (Fujiwara *et al.*, 2011; Ito *et al.*, 2011). The site of large slip near the trench (Fig. 2) almost agrees with the source area of the primary crests of the tsunami observed by the OBPGs and GPS buoys in deep sea (Hayashi *et al.*, 2011).

## 3. Coulomb Stress Changes

We use the slip distributions obtained in the preceding section to calculate the ΔCFF for the aftershock focal mechanisms determined by Nettles *et al.* (2011) (Fig. 3). The aftershock data consists of 81 events ($M > 5.5$) that occurred within 25 days following the mainshock. The aftershock sequence extends over a portion of the plate boundary more than 500 km long, and exhibits an unusual diversity of faulting geometries. We use the centroid hypocenters and the best double-couple solutions determined by Nettles *et al.* (2011) to calculate the Coulomb stress change. The errors in the focal depths are estimated to be less than 2.5 km for events whose focal depths are freely determined (Nettles *et al.*, 2011). For about one-third of the events, the centroid hypocenters are determined with focal depths fixed in a range of 12–16 km. As a whole, the focal depths of the aftershocks near the trench are distributed in a range of 10–20 km. Since the fault planes are not identified, we calculate the Coulomb stress change for each of the two nodal planes, and regard an aftershock as being positively stressed if the Coulomb stress change for either one of the nodal planes has a positive value. Based on the results of Toda *et al.* (2011), we assume an apparent coefficient of friction of 0.4. The rigidity is assumed to be 40 GPa.

We emphasize here that the Coulomb stress changes shown in Fig. 3 are those calculated for the fault model in which the plate boundary is shifted upward by 6.5 km. The relationship between the original plate boundary and the shifted one is exhibited on the vertical cross-section in Fig. 4. In the previous section, the displacements due to the mainshock slip are calculated for the fault model with the upper end of the plate boundary placed at a depth of 6.5 km. However, when we use this model, we find that the Coulomb stress changes, for most of the aftershocks in the outer rise, are negatively stressed. Before describing the results shown in Fig. 3, we first explain the reason why we prefer the Coulomb stress change calculated for the model with the upper end of the fault shifted toward the free surface.

In Figs. 4(a) and 4(b), we compare the Coulomb stress change calculated for the original plate boundary with that calculated for the elevated plate boundary. The Coulomb stress changes are those calculated for the slip distribution with the center of slip close to the trench (Fig. 1(b)). Receiver faults are assumed to be of DDE-type previously defined by Hiratsuka and Sato (2011) (see figures 3 and 4 of that paper). In the area close to the trench where the dip of the plate interface is very shallow, the receiver faults almost agree with the normal faults dipping at an angle of 45°. As shown in Fig. 4(a), for the case where the upper end of the fault is situated at a depth of 6.5 km, the shallow portion close to the trench is dominated by negative ΔCFF values. Since most of the normal-fault aftershocks in the outer rise have focal depths of 10–20 km (Nettles *et al.*, 2011), they fall within the domain of negative ΔCFF. For the case where the upper end of the fault is shifted upward to the free surface, the area close to the trench is dominated by positive values at all depths (Fig. 4(b)). For this case, we evaluate the Coulomb stress changes for the aftershocks by shifting also their focal depths upward by 6.5 km. As a result, the normal-fault aftershocks in the outer rise fall within the positively-stressed domain. Since the sea bed is overlain by a thick water layer instead of a solid body in the offshore area surrounding the trench, we consider that the model with the upper end of the fault situated at the free surface is preferable for predicting the deformation close to the trench. As it goes away from the trench towards the land, the ΔCFF distribution calculated for the model with the upper end of the fault at the free surface is similar to that calculated for the model with the upper end of the fault at the depth of 6.5 km. Therefore, we consider that the model with the upper end of the fault at the free surface can be used for evaluating the Coulomb stress change for all the aftershocks distributed from the trench to the land.

Now we describe the difference in the Coulomb stress change between the slip distributions with the center of slip distant from the trench and close to the trench. For the slip distribution with the center of slip distant from the trench, 69% of the aftershocks are positively stressed (Fig. 3(a)). A higher score of 85% is achieved by the slip distribution with the center of slip close to the trench (Fig. 3(b)). For this model, most of the aftershocks surrounding the center of slip are positively stressed. In contrast, for the model with the center of slip distant from the trench, several normal-fault aftershocks close to the line C–D are calculated to be negatively stressed. In order for the change in the stress field due to the mainshock to be consistent with these normal-faulting events, the center of slip needs to be close to the trench. This demonstrates the capability of the Coulomb stress changes to help constrain the slip distribution which may be difficult to determine from other available data (Seeber and Armbruster, 2000).

Although the slip distribution with the center of slip close

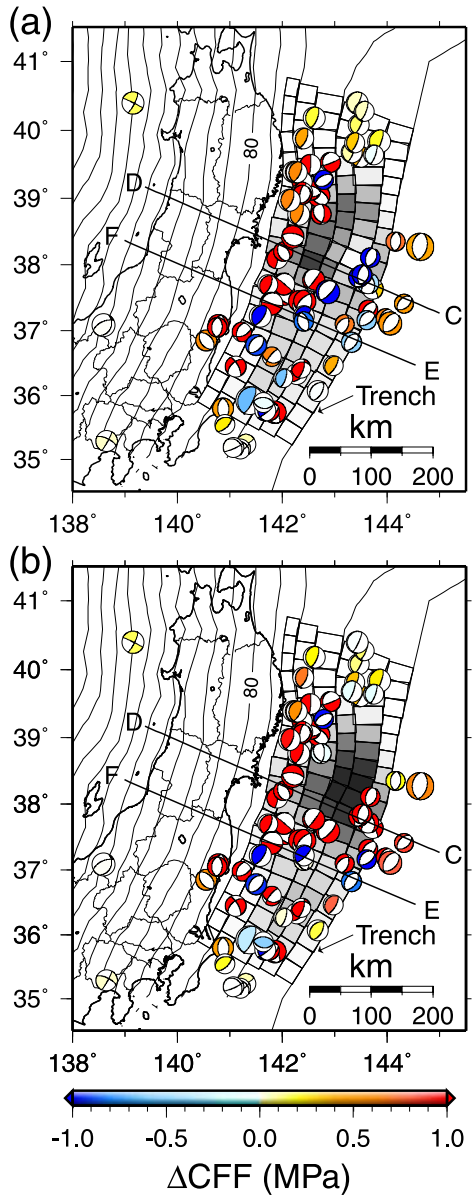


Fig. 3. (a) ΔCFF calculated for the slip distribution with the center of slip distant from the trench (Fig. 1(a)). The colors of the focal mechanisms indicate the ΔCFF values. The larger of the ΔCFF values for the two nodal planes is shown. (b) ΔCFF calculated for the slip distribution with the center of slip close to the trench (Fig. 1(b)). The lines C–D and E–F indicate the locations of ΔCFF profiles shown in Fig. 4.

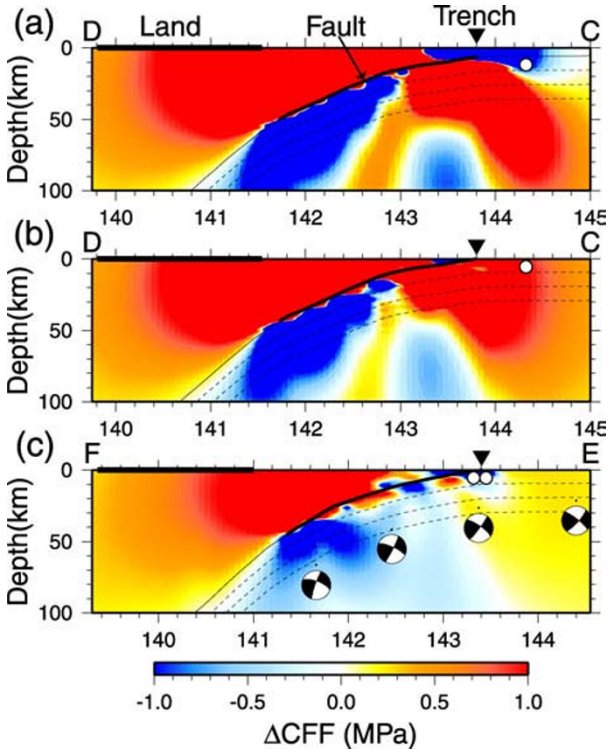


Fig. 4. Cross-sectional views of ΔCFF for receiver faults of down-dip extension (DDE) type previously defined by Hiratsuka and Sato (2011) are shown for the profiles C–D and E–F in Fig. 3. They are calculated for the slip distribution with the center of slip close to the trench (Fig. 1(b)). In the panels (a) and (b), ΔCFF calculated for the model with the upper end of the fault situated at a depth of 6.5 km (a), and with the upper end of the fault situated at the free surface (b), are compared. The open circle indicates the event in the outer rise lying on the line C–D in Fig. 3. The focal depth of the aftershock in (b) is shifted upwards by 6.5 km relative to that shown in (a). (c) ΔCFF along the line E–F calculated for the model with the upper end of the fault placed at the free surface. The open circles indicate the two negatively-stressed normal-fault aftershocks near the trench close to the line E–F in Fig. 3. The mechanism diagrams of receiver faults are indicated in (c). Here, ΔCFF calculated for the westward dipping faults are shown. The broken lines respectively indicate the positions 10, 20, and 30 km below the plate interface.

to the trench is consistent with most of the normal-fault aftershocks near the trench, we find two negatively-stressed normal-fault aftershocks just beneath the trench close to the line E–F. A couple of aftershocks just north of the two events, which are close to the line C–D, are positively stressed in spite of the similar focal mechanisms and epicenter locations relative to the trench. The aftershocks close to the line C–D have a focal depth of 15–20 km while the negatively-stressed aftershocks close to the line E–F have a focal depth of 10–15 km (Nettles *et al.*, 2011). These focal depths in the range of 10–20 km are consistent with the focal depths of aftershocks beneath the trench determined using OBS observations (Obana *et al.*, 2012). The cross-sectional view of ΔCFF for the hypothetical receiver faults along the line E–F shows that normal-fault aftershocks just beneath the trench are expected to be negatively stressed if the focal depths are less than 20 km (Fig. 4(c)). However, Fig. 4(b) shows that the normal-fault aftershocks beneath the trench is positively stressed at all depths. This difference arises from the fact that the slip on the shallow portion of the fault along the line E–F is much smaller than that along the line C–D. We expect that the two normal-fault aftershocks near the trench close to the line E–F would become positively stressed if the slip on the shallow portion of the fault were sufficiently large like that along the line C–D. If we assume ideally that the earthquakes should always occur in a positively-stressed region, the negatively-stressed aftershocks near the trench suggest that the slip inverted from the GPS-derived displacements is smaller than in reality on the shallow part of the fault close to the line E–F. This demonstrates the possibility that the aftershock focal mechanisms can be used to adjust the slip that was originally determined from other available data, but was difficult to constrain.

For the southern part of the mainshock fault where the

slip is relatively small, the number of negatively-stressed aftershocks increases. This may be ascribed to the difference in the degree of fault heterogeneity between the southern and northern regions. A more complicated fault geometry and pattern of slip in the southern region is suggested by its higher aftershock activity compared with the northern region (Hirose *et al.*, 2011).

## 4. Concluding Remarks

We have investigated the change in the Coulomb stress change for the larger aftershocks of the 2011 Tohoku-Oki earthquake, and found that 85% of the aftershocks are positively stressed for a slip distribution with the center of slip close to the trench. Although we cannot base our arguments on the gain in positively-stressed aftershock mechanisms over that for background earthquakes, as done by Toda *et al.* (2011), we consider that the high percentage of positively stressed aftershocks itself supports the validity of a Coulomb stress triggering hypothesis. Comparing the Coulomb stress changes calculated for the different slip distributions, we find that the aftershock focal mechanisms are most consistent with the Coulomb stress changes calculated for a slip distribution with the center of slip close to the trench. This demonstrates the capability of the Coulomb stress changes to help constrain the slip distribution which may be otherwise difficult to determine. Furthermore, we find another possibility that the Coulomb stress changes can be used to condition the slip that is originally determined using other available data, as exemplified by the case of negatively-stressed normal faults along the line E–F. Since the Coulomb stress changes, for the normal-fault aftershocks near the trench, are strongly dependent on the slip on the shallow portion of the fault, they can be combined with other data to constrain the slip distribution close to the trench more reliably.

One of the important issues of the 2011 Tohoku-Oki earthquake is the area of large slip on the shallow portion of the fault. Although there is compelling evidence for a large slip on the shallow part of plate boundary near the trench at 38N (Fujiwara *et al.*, 2011; Ito *et al.*, 2011), the limited distribution of ocean-bottom observations prevents us from determining the size of the source area of large slip along the trench. This problem may be resolved by further investigation of the relationship between the distribution of normal-fault aftershocks and slip near the trench.

**Acknowledgments.** We thank two anonymous reviewers for reading the manuscript and giving valuable comments that were helpful in the revision of the manuscript. We are grateful to Dr. S. Ozawa and Dr. M. Nettles for providing the data used in this study. We also thank Dr. Y. Okada for providing the source code for calculating the elastic deformation due to dislocation in a half space. The figures are prepared using GMT (Wessel and Smith, 1991).

## References

Altamimi, Z., X. Collilieux, J. Legrand, B. Garayt, and C. Boucher, ITRF 2005: A new release of the international terrestrial reference frame based on time series of station positions and earth orientation parameters, *J. Geophys. Res.*, **112**, B09401, doi:10.1029/2007JB004949, 2007.

Fujii, Y., K. Satake, S. Sakai, M. Shinohara, and T. Kanazawa, Tsunami source of the 2011 off the Pacific coast of Tohoku Earthquake, *Earth Planets Space*, **63**, 815–820, 2011.

Fujiwara, T., S. Kodaira, T. No, Y. Kaiho, Y. Takahashi, and Y. Kaneda, The 2011 Tohoku-Oki earthquake: Displacement reaching the trench axis, *Science*, **334**, 1240, doi:10.1126/science.1211554, 2011.

Hayashi, Y., H. Tsushima, K. Hirata, K. Kimura, and K. Maeda, Tsunami source area of the 2011 off the Pacific coast of Tohoku Earthquake determined from tsunami arrival times at offshore observation stations, *Earth Planets Space*, **63**, 809–813, 2011.

Hiratsuka, S. and T. Sato, Alteration of stress field brought about by the occurrence of the 2011 off the Pacific coast of Tohoku Earthquake ($M_w$ 9.0), *Earth Planets Space*, **63**, 681–685, 2011.

Hirose, F., K. Miyaoka, N. Hayashimoto, T. Yamazaki, and M. Nakamura, Outline of the 2011 off the Pacific coast of Tohoku Earthquake ($M_w$ 9.0)—Seismicity: foreshocks, mainshock, aftershocks, and induced activity—, *Earth Planets Space*, **63**, 513–518, 2011.

Ito, Y., T. Tsuji, Y. Osada, M. Kido, D. Inazu, Y. Hayashi, H. Tsushima, R. Hino, and H. Fujimoto, Frontal wedge deformation near the source region of the 2011 Tohoku-Oki earthquake, *Geophys. Res. Lett.*, **38**, L00G05, doi:10.1029/2011GL048355, 2011.

Nakagawa, T. and Y. Oyanagi, Program system SALS for nonlinear least squares fitting in experimental sciences, in *Proceedings of Recent Developments in Statistical Inference and Data Analysis*, edited by K. Matusita, pp. 221–225, North Holland Publishing Company, Amsterdam, 1980.

Nettles, M., G. Ekström, and H. C. Koss, Centroid-moment-tensor analysis of the 2011 off the Pacific coast of Tohoku Earthquake and its larger foreshocks and aftershocks, *Earth Planets Space*, **63**, 519–523, 2011.

Obana, K., G. Fujie, T. Takahashi, Y. Yamamoto, Y. Nakamura, S. Kodaira, N. Takahashi, Y. Kaneda, and M. Shinohara, Normal-faulting earthquakes beneath the outer slope of the Japan Trench after the 2011 Tohoku earthquake: Implications for the stress regime in the incoming Pacific plate, *Geophys. Res. Lett.*, **39**, L00G24, doi:10.1029/2011GL050399, 2012.

Okada, Y., Internal deformation due to shear and tensile faults in a half-space, *Bull. Seismol. Soc. Am.*, **82**, 1018–1040, 1992.

Ozawa, S., T. Nishimura, H. Suito, T. Kobayashi, M. Tobita, and T. Imakire, Coseismic and postseismic slip of the 2011 magnitude-9 Tohoku-Oki earthquake, *Nature*, **475**, 373–376, doi:10,1038/nature10227, 2011.

Sato, M., T. Ishikawa, N. Ujihara, S. Yoshida, M. Fujita, M. Mochizuki, and A. Asada, Displacement above the hypocenter of the 2011 Tohoku-Oki earthquake, *Science*, **332**, 1395, doi:10.1126/Science.1207401, 2011.

Seeber, L. and J. G. Armbruster, Earthquakes as beacons of stress change, *Nature*, **407**, 69–72, 2000.

Takeuchi, M., T. Sato, and T. Shinbo, Stress due to the interseismic back slip and its relation with the focal mechanisms of earthquakes occurring in the Kuril and northeastern Japan arcs, *Earth Planets Space*, **60**, 549–557, 2008.

Toda, S., J. Lin, and R. S. Stein, Using the 2011 $M_w$ 9.0 off the Pacific coast of Tohoku Earthquake to test the Coulomb stress triggering hypothesis and to calculate faults brought closer to failure, *Earth Planets Space*, **63**, 725–730, 2011.

Wessel, P. and W. H. F. Smith, Free software helps map and display data, *Eos Trans. AGU*, **72**, 441, 1991.

T. Sato (e-mail: tamao@cc.hirosaki-u.ac.jp), S. Hiratsuka, and J. Mori